INTERNATIONAL JOURNAL OF
ENERGY AND ENVIRONMENT

Volume 2, Issue 2, 2011 pp.211-218
Journal homepage: www.IJEE.IEEFoundation.org

Exergoeconomic performance optimization of an endoreversible intercooled regenerated Brayton cogeneration plant
Part 2: Heat conductance allocation and pressure ratio optimization

Bo Yang, Lingen Chen, Fengrui Sun

Postgraduate School, Naval University of Engineering, Wuhan 430033, P. R. China.

Abstract
Finite time exergoeconomic performance of an endoreversible intercooled regenerative Brayton cogeneration plant is optimized based on the model which is established using finite time thermodynamic in Part 1 of this paper. It is found that the optimal heat conductance allocation of the regenerator is zero. When the total pressure ratio and the heat conductance allocation of the regenerator are fixed, it is shown that there exist an optimal intercooling pressure ratio, and a group of optimal heat conductance allocations among the hot-, cold- and consumer-side heat exchangers and the intercooler, which correspond to a maximum dimensionless profit rate. When the total pressure ratio is variable, there exists an optimal total pressure ratio which corresponds to a double-maximum dimensionless profit rate, and the corresponding exergetic efficiency is obtained. The effects of the total heat exchanger conductance, price ratios and the consumer-side temperature on the double-maximum dimensionless profit rate and the corresponding exergetic efficiency are discussed. It is found that there exists an optimal consumer-side temperature which corresponds to a thrice-maximum dimensionless profit rate.

Keywords: Endoreversible intercooled regenerative Brayton cogeneration plant, Profit rate, Exergetic efficiency, Finite time thermodynamics, Heat conductance allocation, Pressure ratio, Optimization.

1. Introduction
A thermodynamic model of an endoreversible intercooled regenerative Brayton cogeneration plant is established using finite time thermodynamic in Part 1 [1] of this paper based on the Refs. [2-8]. The analytical formulae about the relations among the dimensionless profit rate, exergetic efficiency and the effectivenesses of the five heat exchangers, the intercooling pressure ratio and the total pressure ratio are derived. The dimensionless profit rate will be optimized by using the similar principle and method used in various intercooled regenerative Brayton cycles [9-17] in which the power, efficiency and power density were taken as the optimization objectives, respectively.
The exergoeconomic performance optimization is performed by searching the optimal intercooling pressure ratio and the optimal heat conductance allocations among the hot-, cold- and consumer-side heat

exchangers, the intercooler and the regenerator for the fixed total pressure ratio. When the total pressure ratio is variable, the performance optimization is performed further by searching the optimal total pressure ratio. The effects of the ratio of the hot-side heat reservoir temperature to environment temperature, the total heat exchanger conductance, price ratios and the consumer-side temperature parameter on the exergoeconomic performance are studied.

2. Numerical examples

According to equation (19) in Part 1 of this paper, the dimensionless profit rate ($\overline{\Pi}$) of the endoreversible intercooled regenerative Brayton cogeneration plant coupled to constant- temperature heat reservoirs is the function of the intercooling pressure ratio (π_1), the total pressure ratio (π) and the five heat conductances (U_H , U_L, U_K, U_I, U_R) when the other boundary condition parameters (T_H, T_L, T_I, T_K, C_{wf}) are fixed. Equation (19) includes the optimal results of some Brayton cogeneration cycles. When $U_R = 0$, one can obtain the results of an endoreversible intercooled Brayton cogeneration cycle. When $U_I = 0$, one can obtain the results of an endoreversible regenerated Brayton cogeneration cycle [8]. When $U_R = 0$ and $U_I = 0$, one can obtain the results of an endoreversible simple Brayton cogeneration cycle [7].

In practical design, π_1, π, U_H , U_L, U_K, U_I, U_R are changeable and the cost per unit of heat conductance may be different for each heat exchanger because different materials may be used. To simplify the problem, the constraint on total heat exchanger conductance is used for the performance optimization. Assuming that the total heat exchanger conductance ($U_T = U_H + U_L + U_K + U_I + U_R$) is fixed, a group of heat conductance allocations are defined as:

$$u_h = U_H / U_T, u_l = U_L / U_T, u_k = U_K / U_T, u_i = U_I / U_T, u_r = U_R / U_T \tag{1}$$

Additionally, one has the constraints:

$$0 < u_h < 1, 0 < u_l < 1, 0 < u_k < 1, 0 < u_i < 1, 0 < u_r < 1, u_h + u_l + u_k + u_i + u_r = 1 \tag{2}$$

For the fixed π and π_1, the optimization can be performed by searching the optimal heat conductance allocations ($(u_h)_{\overline{\Pi}_{opt}}$, $(u_l)_{\overline{\Pi}_{opt}}$, $(u_k)_{\overline{\Pi}_{opt}}$, $(u_i)_{\overline{\Pi}_{opt}}$, $(u_r)_{\overline{\Pi}_{opt}}$) which lead to an optimal dimensionless profit rate ($\overline{\Pi}_{opt}$). One can always obtain $(u_r)_{\overline{\Pi}_{opt}} = 0$. The reason is that for the Brayton cycle discussed herein, the regeneration has little effect on the optimal dimensionless profit rate.

Another method is adopted herein: when u_r and π are fixed, the optimization can be performed by searching the other four optimal heat conductance allocations ($(u_h)_{\overline{\Pi}_{\max}}$, $(u_l)_{\overline{\Pi}_{\max}}$, $(u_k)_{\overline{\Pi}_{\max}}$, $(u_i)_{\overline{\Pi}_{\max}}$) and the optimal intercooling pressure ratio ($(\pi_1)_{\overline{\Pi}_{\max}}$) which lead to a maximum dimensionless profit rate ($\overline{\Pi}_{\max}$).

To search the optimal values of u_h, u_l, u_k, u_i and π_1, the numerical calculations are provided by using the optimization toolbox of Matlab 7.1. In the calculations, four temperature ratios are defined: $\tau_1 = T_H / T_0$, $\tau_2 = T_L / T_0$, $\tau_3 = T_I / T_0$ and $\tau_4 = T_K / T_0$, and $U_T = 10 kW/K$, $u_r = 0.1$, $k = 1.4$, $C_{wf} = 1.0 kW/K$, $\tau_2 = \tau_3 = 1$, $\tau_4 = 1.2$ are set. According to analysis in Ref. [18], $a = 10$ and $b = 6$ are set.

2.1 Optimal dimensionless profit rate and corresponding exergetic efficiency

Assuming that $\pi = 18$ $(1 \le \pi_1 \le 18)$. Figure 1 shows the characteristic of the optimal dimensionless profit rate ($\overline{\Pi}_{opt}$) versus π_1 for different τ_1. Figure 2 shows the characteristics of the optimal heat conductance allocations ($(u_j)_{\overline{\Pi}_{opt},\ j=h,l,k,i}$) and the corresponding exergetic efficiency ($(\eta_{ex})_{\overline{\Pi}_{opt}}$) versus π_1 with $\tau_1 = 5.0$.

It can be seen from Figure 1 that $\overline{\Pi}_{opt}$ increases with the increase of τ_1. There exists an optimal value of intercooling pressure ratio ($(\pi_1)_{\overline{\Pi}_{\max}}$) which leads to a maximum dimensionless profit rate ($\overline{\Pi}_{\max}$). The calculation illustrates that when π_1 is increased to a certain value, one has $(u_i)_{\overline{\Pi}_{opt}} = 0$. It can be seen from Figure 2 that with the increase of π_1, $(u_h)_{\overline{\Pi}_{opt}}$ and $(u_k)_{\overline{\Pi}_{opt}}$ decrease first and then increase, $(u_l)_{\overline{\Pi}_{opt}}$

increases and $(u_i)_{\overline{\Pi}_{opt}}$ decreases except that π_1 is very small. The optimal heat conductance allocations which correspond to $\overline{\Pi}_{\max}$ are $(u_j)_{\overline{\Pi}_{\max},\, j=h,l,k,i}$. $(\eta_{ex})_{\overline{\Pi}_{opt}}$ exists a maximum value and a minimum value, and the exergetic efficiency corresponding to $\overline{\Pi}_{\max}$ is $(\eta_{ex})_{\overline{\Pi}_{\max}}$.

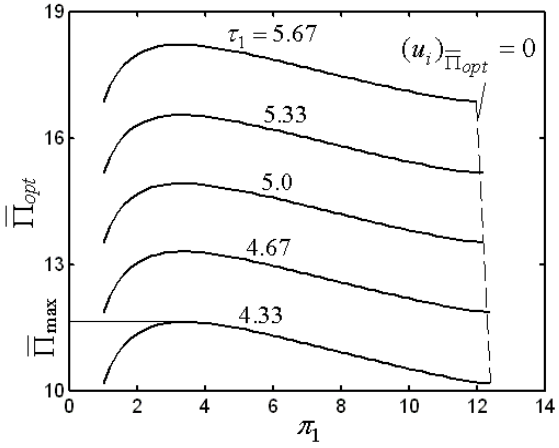

Figure 1. Effect of τ_1 on the characteristic of $(\overline{e_{out}})_{opt}$ versus π_1

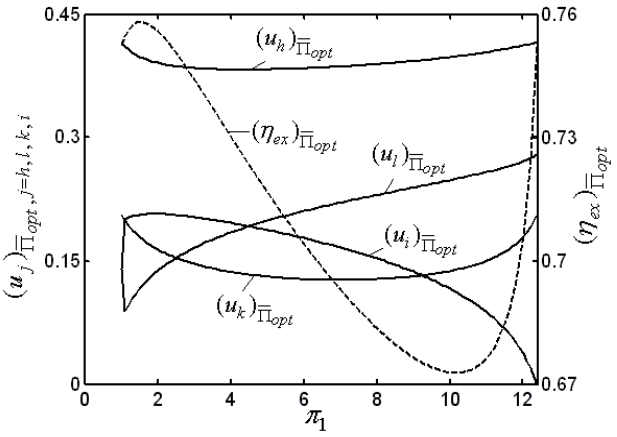

Figure 2. Characteristic of $(u_j)_{\overline{\Pi}_{opt},\, j=h,l,k,i}$ and $(\eta_{ex})_{\overline{\Pi}_{opt}}$ versus π_1

2.2 Maximum dimensionless profit rate and corresponding exergetic efficiency

Figures 3 and 4 show the characteristics of the maximum dimensionless profit rate ($\overline{\Pi}_{\max}$) and the corresponding exergetic efficiency ($(\eta_{ex})_{\overline{\Pi}_{\max}}$), the optimal heat conductance allocations ($(u_j)_{\overline{\Pi}_{\max},\, j=h,l,k,i}$) and optimal intercooling pressure ratio ($(\pi_1)_{\overline{\Pi}_{\max}}$) versus π with $\tau_1 = 5.0$, respectively. It can be seen from Figure 3 that there exists an optimal value of total pressure ratio ($\pi_{\overline{\Pi}_{\max,2}}$) which lead to a double-maximum dimensionless profit rate ($\overline{\Pi}_{\max,2}$), and $\overline{\Pi}_{\max}$ changes slowly when π is large. $(\eta_{ex})_{\overline{\Pi}_{\max}}$ exists an extremum with respect to π, and the exergetic efficiency corresponding to $\overline{\Pi}_{\max,2}$ is $(\eta_{ex})_{\overline{\Pi}_{\max,2}}$. It can be seen from Figure 4 that with the increase of π, $(u_h)_{\overline{\Pi}_{\max}}$ and $(u_k)_{\overline{\Pi}_{\max}}$ decrease, $(u_i)_{\overline{\Pi}_{\max}}$, $(u_l)_{\overline{\Pi}_{\max}}$ and $(\pi_1)_{\overline{\Pi}_{\max}}$ increase. The optimal heat conductance allocations corresponding to $\overline{\Pi}_{\max,2}$ are $(u_j)_{\overline{\Pi}_{\max,2},\, j=h,l,k,i}$.

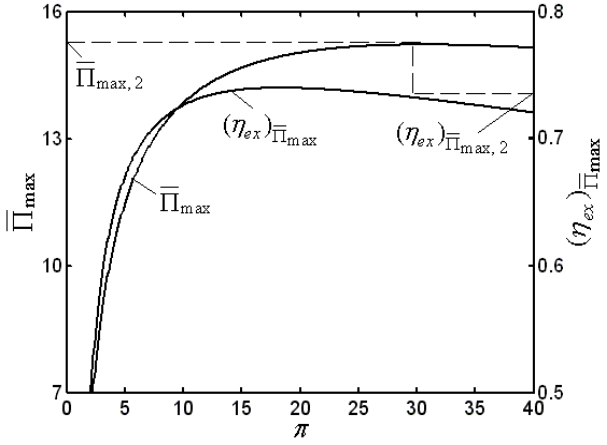

Figure 3. Characteristics of $\overline{\Pi}_{\max}$ and $(\eta_{ex})_{\overline{\Pi}_{\max}}$ versus π

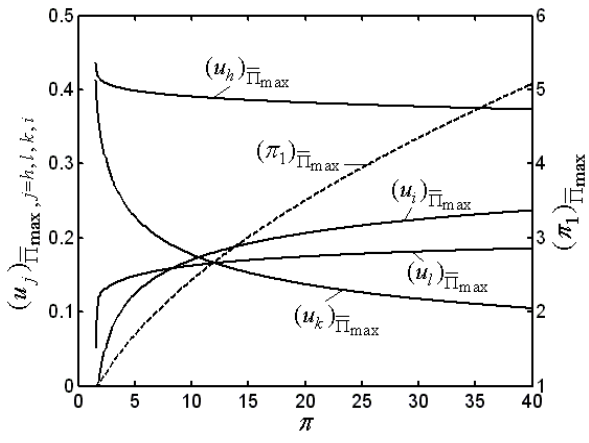

Figure 4. Characteristics of $(u_j)_{\overline{\Pi}_{\max}}$, $_{j=h,l,k,i}$ and $(\pi_1)_{\overline{\Pi}_{\max}}$ versus π

3. Effects of total heat conductance, price ratios and consumer-side temperature

Figures 5 and 6 show the characteristics of the double-maximum dimensionless profit rate ($\overline{\Pi}_{\max,2}$) and the corresponding exergetic efficiency ($(\eta_{ex})_{\overline{\Pi}_{\max,2}}$), the optimal heat conductance allocations ($(u_j)_{\overline{\Pi}_{\max,2},\ j=h,l,k,i}$) and the optimal total pressure ratio ($\pi_{\overline{\Pi}_{\max,2}}$) versus U_T with $\tau_1 = 5.0$, respectively. It can be seen from Figure 5 that $\overline{\Pi}_{\max,2}$ and $(\eta_{ex})_{\overline{\Pi}_{\max,2}}$ increase with the increase of U_T, and increase slowly when U_T is large. It can be seen from Figure 6 that with the increase of U_T, $(u_h)_{\overline{\Pi}_{\max,2}}$ decreases, $(u_i)_{\overline{\Pi}_{\max,2}}$ and $\pi_{\overline{\Pi}_{\max,2}}$ increase, and $(u_l)_{\overline{\Pi}_{\max,2}}$ and $(u_k)_{\overline{\Pi}_{\max,2}}$ decrease first and then increase.

Figures7 and 8 show the characteristics of $\overline{\Pi}_{\max,2}$ and $(\eta_{ex})_{\overline{\Pi}_{\max,2}}$, $(u_j)_{\overline{\Pi}_{\max,2},\ j=h,l,k,i}$ and $\pi_{\overline{\Pi}_{\max,2}}$ versus price ratio (a), respectively. It can be seen from Figure 7 that with the increase of a, $\overline{\Pi}_{\max,2}$ increases, and $(\eta_{ex})_{\overline{\Pi}_{\max,2}}$ increases first and then decreases. It can be seen from Figure 8 that with the increase of a, $(u_h)_{\overline{\Pi}_{\max,2}}$ changes slightly, $(u_k)_{\overline{\Pi}_{\max,2}}$ decreases, and $(u_i)_{\overline{\Pi}_{\max,2}}$, $(u_l)_{\overline{\Pi}_{\max,2}}$, and $\pi_{\overline{\Pi}_{\max,2}}$ increase.

Figures9 and 10 show the characteristics of $\overline{\Pi}_{\max,2}$ and $(\eta_{ex})_{\overline{\Pi}_{\max,2}}$, $(u_j)_{\overline{\Pi}_{\max,2},\ j=h,l,k,i}$ and $\pi_{\overline{\Pi}_{\max,2}}$ versus price ratio (b), respectively. It can be seen from Figure 9 that $\overline{\Pi}_{\max,2}$ and $(\eta_{ex})_{\overline{\Pi}_{\max,2}}$ increase with the increase of b. It can be seen from Figure 10 that with the increase of b, $(u_h)_{\overline{\Pi}_{\max,2}}$ changes slightly, $(u_k)_{\overline{\Pi}_{\max,2}}$ increases, $(u_l)_{\overline{\Pi}_{\max,2}}$ decreases, and $(u_i)_{\overline{\Pi}_{\max,2}}$ and $\pi_{\overline{\Pi}_{\max,2}}$ decrease approximately linearly.

Figures 11 and 12 show the characteristics of $\overline{\Pi}_{\max,2}$ and $(\eta_{ex})_{\overline{\Pi}_{\max,2}}$, $(u_j)_{\overline{\Pi}_{\max,2},\ j=h,l,k,i}$ and $\pi_{\overline{\Pi}_{\max,2}}$ versus τ_4, respectively. It can be seen from Figure 11 that there exists an optimal consumer-side temperature which leads to a thrice-maximum dimensionless profit rate. $(\eta_{ex})_{\overline{\Pi}_{\max,2}}$ also exists an extremum with respect to τ_4. It can be seen from Figure 12 that with the increase of τ_4, $(u_h)_{\overline{\Pi}_{\max,2}}$ changes slightly, $(u_k)_{\overline{\Pi}_{\max,2}}$ decreases, $(u_l)_{\overline{\Pi}_{\max,2}}$ increases, and $(u_i)_{\overline{\Pi}_{\max,2}}$ and $\pi_{\overline{\Pi}_{\max,2}}$ decrease first and then increase.

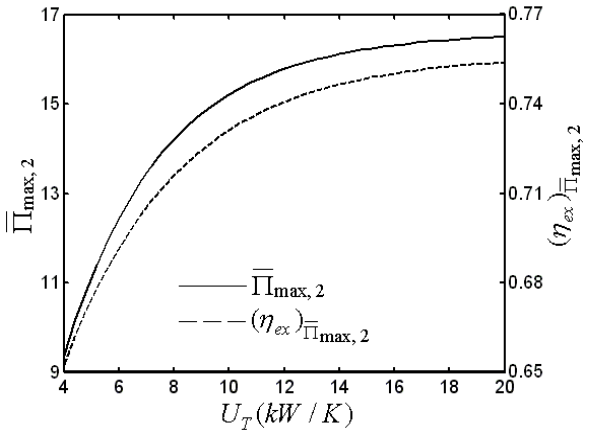

Figure 5. Characteristics of $\overline{\Pi}_{\max,2}$ and $(\eta_{ex})_{\overline{\Pi}_{\max,2}}$ versus U_T

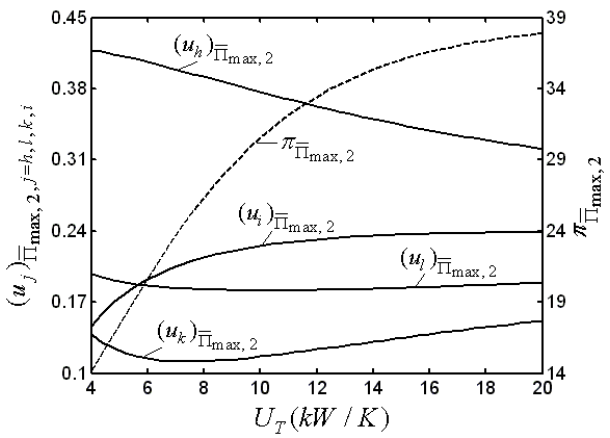

Figure 6. Characteristics of $(u_j)_{\overline{\Pi}_{\max,2},\ j=h,l,k,i}$ and $\pi_{\overline{\Pi}_{\max,2}}$ versus U_T

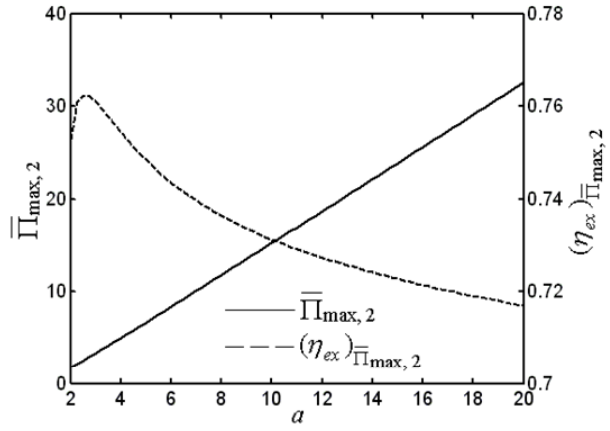

Figure 7. Characteristics of $\overline{\Pi}_{\max,2}$ and $(\eta_{ex})_{\overline{\Pi}_{\max,2}}$ versus a

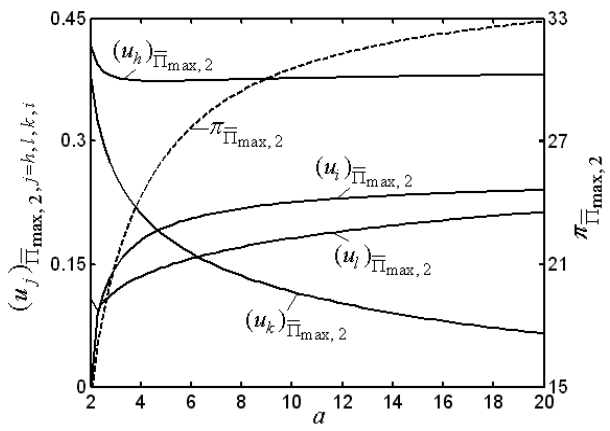

Figure 8. Characteristics of $(u_j)_{\overline{\Pi}_{\max,2},\ j=h,l,k,i}$ and $\pi_{\overline{\Pi}_{\max,2}}$ versus a

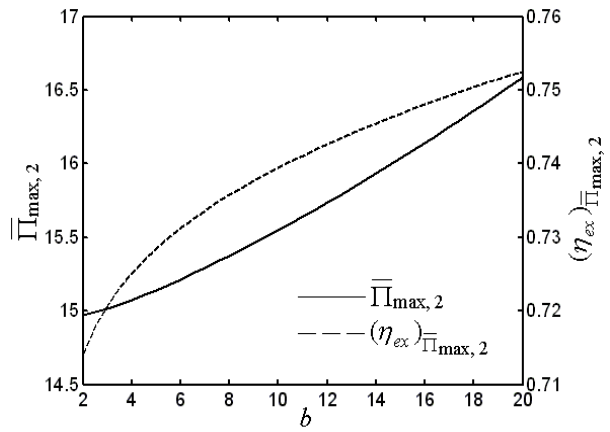

Figure 9. Characteristics of $\overline{\Pi}_{\max,2}$ and $(\eta_{ex})_{\overline{\Pi}_{\max,2}}$ versus b

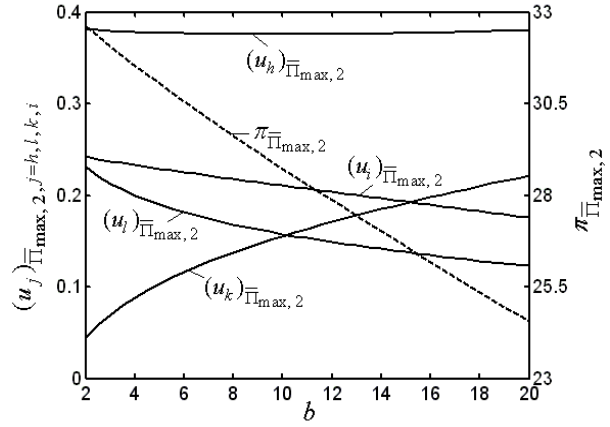

Figure 10. Characteristics of $(u_j)_{\overline{\Pi}_{\max,2},\ j=h,l,k,i}$ and $\pi_{\overline{\Pi}_{\max,2}}$ versus b

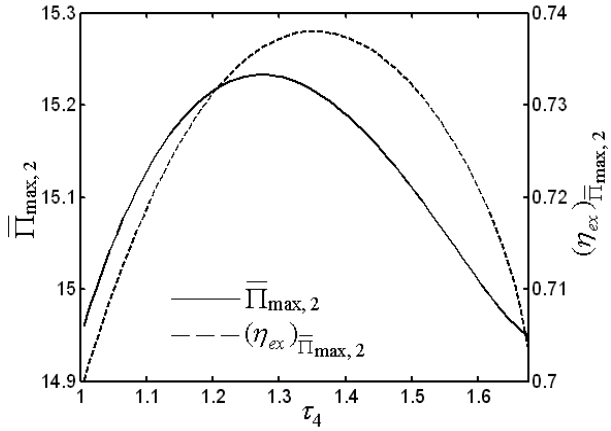

Figure 11. Characteristics of $\overline{\Pi}_{\max,2}$ and $(\eta_{ex})_{\overline{\Pi}_{\max,2}}$ versus τ_4

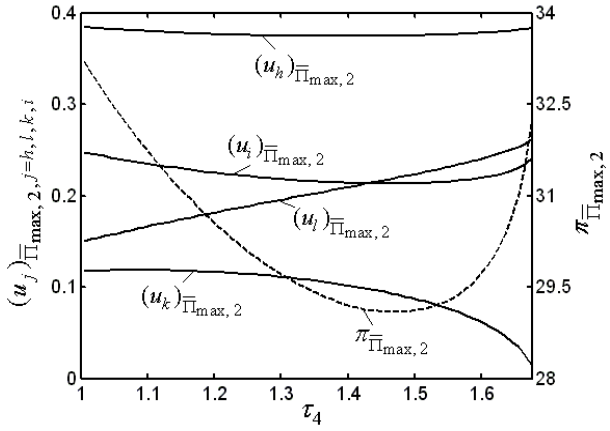

Figure 12. Characteristics of $(u_j)_{\overline{\Pi}_{\max,2},\ j=h,l,k,i}$ and $\pi_{\overline{\Pi}_{\max,2}}$ versus τ_4

4. Conclusion

Finite time exergoeconomic performance of a heat and power cogeneration plant model composed of an endoreversible intercooled regenerative Brayton closed-cycle coupled to constant-temperature heat reservoirs is optimized by numerical examples. The main conclusions are as follows:

(1) When the optimization is performed with respect to the five heat conductance allocations of the hot-, cold- and consumer-side heat exchangers, the intercooler and the regenerator for a fixed total heat exchanger conductance, the optimal heat conductance allocation of the regenerator is always zero in the operation state of optimal dimensionless profit rate.

(2) When the heat conductance allocation of the regenerator and the total pressure ratio are fixed, there exist an optimal intercooling pressure ratio and a group of optimal heat conductance allocations of the hot-, cold- and consumer-side heat exchangers and the intercooler which lead to a maximum dimensionless profit rate. When the total pressure ratio is variable, there exists an optimal total pressure ratio which leads to a double-maximum dimensionless profit rate. Also the exergetic efficiency corresponding to the maximum dimensionless profit rate is obtained.

(3) The effects of total heat exchanger conductance, price ratios and consumer-side temperature on the double-maximum dimensionless profit rate and the corresponding exergetic efficiency, the optimal heat conductance allocations and the optimal total pressure ratio are discussed in detail. One can find that the larger the total heat exchanger conductance and the price ratios, the better the exergoeconomic performance. There exists an optimal consumer-side temperature which leads to a thrice-maximum dimensionless profit rate.

Acknowledgements

This paper is supported by The National Natural Science Foundation of P. R. China (Project No. 10905093), The Program for New Century Excellent Talents in University of P. R. China (Project No. NCET-04-1006) and The Foundation for the Author of National Excellent Doctoral Dissertation of P. R. China (Project No. 200136).

Nomenclature

a	price ratio of power output to exergy input rate
b	price ratio of thermal exergy output rate to exergy input rate
C	heat capacity rate (kW / K)
k	ratio of the specific heats
T	temperature (K)
U	heat conductance (kW / K)
u_h	hot-side heat conductance allocation
u_i	heat conductance allocation of the intercooler
u_k	consumer-side heat conductance allocation
u_l	cold-side heat conductance allocation
u_r	heat conductance allocation of the regenerator

Greek symbols

η	efficiency
Π	profit rate (*dollar*)
π_1	intercooling pressure ratio
π	total pressure ratio
τ_1	ratio of the hot-side heat reservoir temperature to environment temperature
τ_2	ratio of the cold-side heat reservoir temperature to environment temperature
τ_3	ratio of the intercooling fluid temperature to environment temperature
τ_4	ratio of the consumer-side temperature to environment temperature

Subscripts

ex	Exergy
H	hot-side
I	intercooler

K	consumer-side
L	cold-side
max	maximum
opt	optimal
R	regenerator
T	total
wf	working fluid
0	Ambient
$^-$	dimensionless

References

[1] Chen L, Yang B, Sun F. Exergoeconomic performance optimization of an endoreversible intercooled regenerated Brayton cogeneration plant. Part 1: thermodynamic model and parameter analyses. Int. J. Energy and Environment, 2011, 2(2): 199-210.

[2] Yilmaz T. Performance optimization of a gas turbine-based cogeneration system. J. Phys. D: Appl. Phys., 2006, 39(11): 2454-2458.

[3] Yilmaz T, Bayraktar S, Tasci F. Efficiency optimisation of gas turbine based cogeneration cycle. J. Energy Instit., 2008, 81(2): 110-113.

[4] Hao X, Zhang G. Maximum useful energy-rate analysis of an endoreversible Joule-Brayton cogeneration cycle. Appl. Energy, 2007, 84(11): 1092-1101.

[5] Hao X, Zhang G. Exergy optimisation of a Brayton cycle-based cogeneration plant. Int. J. Exergy, 2009, 6(1): 34-48.

[6] Ust Y, Sahin B, Yilmaz T. Optimization of a regenerative gas-turbine cogeneration system based on a new exergetic performance criterion: exergetic performance coefficient. Proc. IMechE, Part A: J. Power and Energy, 2007, 221(4): 447-458.

[7] Tao G, Chen L, Sun F, Wu C. Exergoeconomic performance optimization for an endoreversible simple gas turbine closed-cycle cogeneration plant. Int. J. Ambient Energy, 2009, 30(3): 115-124.

[8] Tao G, Chen L, Sun F. Exergoeconomic performance optimization for an endoreversible regenerative gas turbine closed-cycle cogeneration plant. Riv. Mex. Fis., 2009, 55(3): 192-200.

[9] Wang W, Chen L, Sun F, Wu C. Power optimization of an endoreversible intercooled regenerated Brayton cycle. Int. J. Thermal Sci., 2005, 44(1): 89-94.

[10] Wang W, Chen L, Sun F, Wu C. Power optimization of an endoreversible closed intercooled regenerated Brayton cycle coupled to variable-temperature heat reservoirs. Appl. Energy, 2005, 82(2): 181-195.

[11] Wang W, Chen L, Sun F, Wu C. Optimal heat conductance distribution and optimal intercooling pressure ratio for power optimization of an irreversible closed intercooled regenerated Brayton cycle. J. Energy Instit., 2006, 79(2): 116-119.

[12] Wang W, Chen L, Sun F, Wu C. Power optimization of an irreversible closed intercooled regenerated Brayton cycle coupled to variable-temperature heat reservoirs. Appl. Therm. Eng., 2005, 25(8-9): 1097-1113.

[13] Wang W, Chen L, Sun F, Wu C. Efficiency optimization of an irreversible closed intercooled regenerated gas-turbine cycle. Proc. IMechE, Part A: J. Power and Energy, 2006, 220(A6): 551-558.

[14] Chen L, Wang J, Sun F. Power density optimisation of an endoreversible closed intercooled regenerated Brayton cycle. J. Energy Instit., 2007, 80(2): 105-109.

[15] Chen L, Wang J, Sun F, Wu C. Power density optimization of an endoreversible closed variable-temperature heat reservoir intercooled regenerated Brayton cycle. Int. J. Ambient Energy, 2006, 27(2): 99-112.

[16] Chen L, Wang J, Sun F. Power density analysis and optimization of an irreversible closed intercooled regenerated Brayton cycle. Math. Comput. Model., 2008, 48(3/4): 527-540.

[17] Chen L, Wang J, Sun F, Wu C. Power density optimization of an irreversible variable-temperature heat reservoir closed intercooled regenerated Brayton cycle. Int. J. Ambient Energy, 2009, 30(1): 9-26.

[18] Fang G, Cai R, Lin R. Analysis on basic parameters in cogeneration cycle with gas turbine and steam turbine. J. Power Engng., 1998, 8(6): 118-124 (in Chinese).

Bo Yang received his BS Degree from the Naval University of Engineering, P R China in 2008. He is pursuing for his MS Degree in power engineering and engineering thermophysics of Naval University of Engineering, P R China. His work covers topics in finite time thermodynamics and technology support for propulsion plants. He is the author or co-author of over 8 peer-refereed papers.

Lingen Chen received all his degrees (BS, 1983; MS, 1986, PhD, 1998) in power engineering and engineering thermophysics from the Naval University of Engineering, P R China. His work covers a diversity of topics in engineering thermodynamics, constructal theory, turbomachinery, reliability engineering, and technology support for propulsion plants. He has been the Director of the Department of Nuclear Energy Science and Engineering and the Director of the Department of Power Engineering. Now, he is the Superintendent of the Postgraduate School, Naval University of Engineering, P R China. Professor Chen is the author or coauthor of over 1050 peer-refereed articles (over 460 in English journals) and nine books (two in English).
E-mail address: lgchenna@yahoo.com; lingenchen@hotmail.com, Fax: 0086-27-83638709 Tel: 0086-27-83615046

Fengrui Sun received his BS Degrees in 1958 in Power Engineering from the Harbing University of Technology, PR China. His work covers a diversity of topics in engineering thermodynamics, constructal theory, reliability engineering, and marine nuclear reactor engineering. He is a Professor in the Department of Power Engineering, Naval University of Engineering, PR China. He is the author or co-author of over 750 peer-refereed papers (over 340 in English) and two books (one in English).